ISSN 1330–0016
CODEN FIZBE7

SCHWINGER-DYSON APPROACH AND GENERALIZED IMPULSE APPROXIMATION FOR THE $\pi^0\gamma^\star\gamma$ TRANSITION

DUBRAVKO KLABUČAR[a] and DALIBOR KEKEZ[b]

[a] *Department of Physics, Faculty of Science, Zagreb University, P.O.B. 162, 10001 Zagreb, Croatia*

[b] *Rudjer Bošković Institute, P.O.B. 1016, 10001 Zagreb, Croatia*

Received 3 March 1999; Accepted 12 July 1999

We review the pion-photon transition form factor calculated in the Schwinger-Dyson approach and an impulse approximation. We present results for it far above the scales presently accessible for measurement, up to 36 GeV^2, and demonstrate agreement with the analytically inferred asymptotic behaviour, for which we also provide a new derivation. We discuss how measurements at Jefferson Lab can provide information on how quarks are dynamically dressed.

PACS numbers: 11.10.St, 13.40.-f, 14.40.Aq, 14.40.-n, 14.40.Gx UDC 539.126
Keywords: Schwinger-Dyson equations, pion-transition form factor

1. Introduction and survey

A modern version of the constituent quark model with many attractive features is one of remarkable achievements of the Schwinger-Dyson (SD) approach (reviewed in Refs. 1 and 2) to the physics of quarks and hadrons. It is well-known that most quark–antiquark bound state approaches have grave problems when they are faced with the electromagnetic processes dominated by Abelian axial anomaly. (See Ref. 3 for a brief review and more references.) However, these problems are resolved in the SD approach thanks to its good chiral properties. In the chiral limit, the axial-anomaly result for $\pi^0(p) \to \gamma(k)\gamma(k')$ transition amplitude

$$T_{\pi^0}(0,0) = \frac{1}{4\pi^2 f_\pi} \tag{1}$$

is reproduced analytically and exactly in this approach [4,5]. The amplitude in Eq. (1) is the limit when both photons are real ($k^2 = k'^2 = 0$), of the general amplitude $T_{\pi^0}(k^2, k'^2)$.

At first, $\pi^0 \to \gamma\gamma^{(\star)}$ processes and other applications were studied in the approach with physically motivated *Ansätze* (e.g., Refs. 5 and 6), instead of the solutions of SD equations (SDE) with specified dynamics. However, the exact evaluation of Abelian axial anomaly in the closed form (1) occurs also in the variant where one actually solves SDE for the quark propagators and, in a consistent approximation and with the same model interaction, Bethe-Salpeter (BS) equations (BSE) for quark-antiquark bound states. This is the consistently coupled SD-BS approach, of which Ref. 7 and references therein provide an elaborated example.

Since the anomaly is independent of hadronic structure, it is essential to note that the relation (1) is successfully reproduced in the SD approach irrespective of what concrete *Ansatz* for the quark propagator

$$S(q) = [A(q^2)\not{q} - B(q^2)]^{-1} \ , \tag{2}$$

is used, or what concrete consistently coupled SD-BS solutions are employed for the dressed quark propagator (2) and the pion $q\bar{q}$ bound-state BS vertex Γ_{π^0}.

The successful treatment of the Abelian axial anomaly is possible in the SD approach because this approach incorporates the dynamical chiral symmetry breaking (DχSB) into the bound states consistently, so that the pion, although constructed as a $q\bar{q}$ bound state, appears as a Goldstone boson in the chiral limit. With that, the bound-state descriptions of mesons are reconciled with chiral requirements stemming both from QCD as underlying fundamental theory, and from phenomenology. The scenario is essentially of the Nambu–Jona-Lasinio (NJL) type, but *without* its low cutoff. Consequently, the quark-antiquark bound state mesons can finally provide adequate descriptions of the processes where the axial anomaly is important (e.g., see Refs. 4, 5, 6, 8, 9, 10 and 3), such as the two-photon processes of light pseudoscalars, of which the $\pi^0 \to \gamma\gamma$ decay is the cleanest example of an anomalous electromagnetic decay.

Having gotten in hands the fully satisfactory result (1) for the $\pi^0 \to \gamma\gamma$, the next thing to explore was its one-off-shell-photon extension $T_{\pi^0}(k^2, 0)$ in the SD approach. Frank et al. [6] studied it using *Ansätze* for dressed quark propagators (2), and then Ref. 9 did it in the consistently coupled SD-BS approach, utilizing the solutions of Ref. 7. However, both papers called for additional studies in two respects. First, both had employed the soft and chiral limit for the pion; *i.e.*, the BS vertex was approximated by its leading, $\mathcal{O}(p^0)$ piece:

$$\Gamma_{\pi^0}(q,p) \approx \Gamma_{\pi^0}(q,0) = \gamma_5 \, \lambda^3 \, \frac{B(q^2)}{f_\pi} \ . \tag{3}$$

(λ^3 is the third Gell-Mann matrix of flavour $SU(3)$.) In addition, Refs. 6 and 9 could compare their results just with then only available data by CELLO [11], at $Q^2 \lesssim 2.5$ GeV^2.

Lately, however, the interest in the form factor $T_{\pi^0}(-Q^2, 0)$ for the transition $\gamma^\star(k)\gamma(k') \to \pi^0(p)$ (where $k^2 = -Q^2 \neq 0$ is the momentum-squared of the spacelike off-shell photon $\gamma^\star$), has again been growing for both experimental (the new CLEO

data [12] and plans for new TJNAF measurements [13]) and theoretical reasons – e.g., see Ref. 14.

At large values of Q^2, the $\gamma^\star\gamma \to \pi^0$ transition form factor should be adequately given by perturbative QCD (pQCD) - e.g., see Refs. 15, 16 and 17. Nevertheless, it is still not quite certain which Q^2 is sufficiently large. For example, according to Refs. 18, just pQCD may still be not quite sufficient even at the highest of the presently accessible momenta, $Q^2 \lesssim 10$ GeV^2. The pQCD approaches start having problems as Q^2 decreases more and more into the nonperturbative domain. Also, see Sec. IV of the recent Ref. 17 for clarifications how such approaches [16] fail to reproduce the anomaly-induced value (1) at $Q^2 = 0$.

On the other hand, the treatment of the axial anomaly is a strong point of the SD approach, as pointed out above. What must then be explored in the coupled SD-BS approach is if the large Q^2 behaviour is satisfactory. In particular, the comparison with the new CLEO data [12] – at Q^2 up to 8 GeV^2 – must be made. Whether the large Q^2 behaviour is satisfactorily close to the data and to the predictions of pQCD is a tricky question for a constituent quark model. Namely, the calculation of the transition form factor carried out in the simple constituent quark model (with the constant light–quark mass parameter m_u), leads to $T_{\pi^0}(-Q^2, 0) \propto (m_u^2/Q^2) \ln^2(Q^2/m_u^2)$ as $Q^2 \to \infty$, which overshoots both the CLEO data and pQCD predictions considerably [14]. This is because of the additional $\ln^2(Q^2)$-dependence on top of the large Q^2 behaviour

$$T_{\pi^0}(-Q^2, 0) = \mathcal{J}\,\frac{f_\pi}{Q^2} \qquad (\mathcal{J} \to \text{const as } Q^2 \to \infty), \tag{4}$$

favoured by pQCD and other QCD-based theoretical predictions such as Refs. 15, 16, 17, 18, 19 and 21 and references therein. Publication of the CLEO data [12] made it clear that the large-Q^2 behaviour (4) is also favoured experimentally [12].

Fortunately, the constituent quark model provided by the SD approach, in which $B(q^2)/A(q^2)$ plays the role of the dynamically generated q^2-dependent mass, has turned out not to suffer from that shortcoming. Namely, we have shown in Ref. 21 that the above asymptotic behaviour (4) is in this approach obtained in the model-independent way.

In this paper, we provide yet another way to obtain the asymptotic $Q^2 \to \infty$ behaviour found in Ref. 21. Predictions for $T_{\pi^0}(-Q^2, 0)$ for finite values of Q^2 can be obtained by picking a definite model for interactions between quarks and obtaining corresponding solutions of the SDE and BSE. In this paper, just as we did in Ref. 21, we use the model of Ref. 7. However, here we give the results over much wider range of Q^2 - see Fig. 1 and the discussion thereof. Comparison with the data reveals in what way more precise measurements at intermediate momenta, feasible at TJNAF, can both give insights in the hadronic structure and provide guidance how to improve presently existing models in the SD-BS approach. In addition, the coupled SD-BS variant of the SD approach (such as that in Ref. 7) can readily be extended and applied beyond the soft and chiral limits [given by Eq. (3)] for the bound-state vertex - e.g., see Refs. 9, 22, 10 and 3. We did this when calculating

$T_{\pi^0}(-Q^2,0)$ in Ref. 21, but here we locate and point out the main reason for the difference between the full calculation of the transition form factor and the one using the the soft and chiral limit approximation (3) for the pion BS vertex.

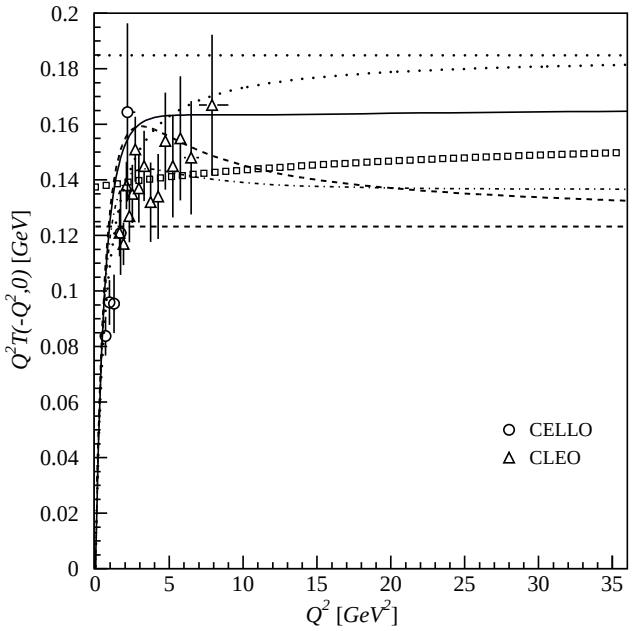

Fig. 1. Our results for $Q^2T_{\pi^0}(-Q^2,0)$ are presented from $Q^2=0$ up to $Q^2=36$ GeV^2. The data presently exist only for $Q^2<10$ GeV^2. CELLO data points are circles and those of CLEO are triangles. The dash-dotted line represents our $Q^2T_{\pi^0}(-Q^2,0)$ evaluated in the chiral and soft limit approximation (3) and only with the BC $qq\gamma$ vertices. Our results without that approximation are depicted by the solid line for the case of the BC vertex, and by the dashed line for the case of the mCP vertex. This latter one gets lower beyond $Q^2\approx 2.5$ GeV^2 and does not yet saturate, but at higher Q^2 ultimately must approach asymptotically $Q^2T_{\pi^0}(-Q^2,0)\to 4f_\pi/3$ for higher Q^2. This limit is also denoted by the dashed line, but the straight one. The Brodsky-Lepage interpolation formula [15] is the dotted curve approaching the (also dotted) straight line denoting the pQCD limiting value $2f_\pi$. The line of empty squares denotes basically the pQCD prediction (but with fixed $N_f=5$) of Ref. 31.

2. Dressed quarks and BS-vertices need dressed $qq\gamma$ vertices

In the coupled SD-BS approach, the BSE for the pion bound-state $q\bar{q}$ vertex $\Gamma_{\pi^0}(q,p)$ employs the dressed quark propagator (2) obtained by solving its SDE. Solving the SDE and BSE in a consistent approximation is crucial (e.g., see Refs.

23, 24, 7, 25 and 22) for obtaining $q\bar{q}$ bound states which are, in the case of light pseudoscalar mesons, simultaneously also the (pseudo-)Goldstone bosons of DχSB.

Following Jain and Munczek [23,24,7], we adopt the ladder-type approximation sometimes called the *improved* [26] or *generalized* [5] ladder approximation (employing bare quark–gluon–quark vertices but dressed propagators). For the gluon propagator we use an effective, (*partially*) modeled one in Landau-gauge [23,24,7], given by $G(-l^2)(g^{\mu\nu} - l^\mu l^\nu/l^2)$. (This Ansatz is often called the "Abelian approximation" [22].) The effective propagator function G is the sum of the perturbative contribution G_{UV} and the nonperturbative contribution G_{IR}: $G(Q^2) = G_{UV}(Q^2) + G_{IR}(Q^2)$, $(Q^2 = -l^2)$. The perturbative part $G_{UV} = (16\pi/3)\alpha_s(Q^2)/Q^2$ is well-known from perturbative QCD, so it is *not* modeled [23,24,7,9,10,3]. As in Refs. 9, 10 and 3, we follow Refs. 23, 24 and 7 and employ the two–loop asymptotic expression for $\alpha_s(Q^2)$. For the modeled, IR part of the gluon propagator, we adopt from Ref. 7 $G_{IR}(Q^2) = (16\pi^2/3)\, a\, Q^2 e^{-\mu Q^2}$, with their parameters $a = (0.387\,\mathrm{GeV})^{-4}$ and $\mu = (0.510\,\mathrm{GeV})^{-2}$. For details of how we solve SDE and BSE, we refer to Refs. 9, 10 and 3. To high accuracy, we reproduce Jain and Munczek's [7] solutions of SDE for the dressed propagators $S(q)$, i.e., the functions $A(q^2)$ and $B(q^2)$, as well as the BS solutions for the four functions comprising the pion bound-state vertex Γ_{π^0}.

The $\pi^0\gamma^\star\gamma$ transition tensor ($T^{\mu\nu}_{\pi^0}$) and scalar (T_{π^0}) amplitudes, related by

$$T^{\mu\nu}_{\pi^0}(k,k') = \varepsilon^{\alpha\beta\mu\nu} k_\alpha k'_\beta T_{\pi^0}(k^2, k'^2) \ , \tag{5}$$

are found in the present paper as in Refs. 9, 10 and 3. That is, the pseudoscalar-vector-vector (PVV) triangle graph is calculated by employing the framework advocated by (for example) Refs. 4, 5, 6, 27 and 8 in the context of electromagnetic interactions of BS bound states, and often called the generalized impulse approximation (GIA) - e.g., by Refs. 6 and 27. To evaluate the triangle graph, we therefore use the *dressed* quark propagator $S(q)$ and the pseudoscalar ($P = \pi^0, \eta_8, \eta_0, \eta_c ...$) meson BS bound–state vertex $\Gamma_P(q,p)$. (See Fig. 1 in Ref. 21, for example.) Equivalently, we can work with the BS-amplitude $\chi_P(q,p) \equiv S(q+p/2)\Gamma_P(q,p)S(q-p/2)$. This is in fact what we do, following Ref. 7.

The third ingredient crucial for GIA's ability to reproduce the correct Abelian anomaly result (1), is employing in the triangle graph appropriately dressed *electromagnetic* vector vertices $\Gamma^\mu(q',q)$, which satisfy the vector Ward–Takahashi identity (WTI) $(q'-q)_\mu\Gamma^\mu(q',q) = S^{-1}(q') - S^{-1}(q)$. Namely, assuming that photons couple to quarks through the bare vertex γ^μ would be inconsistent with our quark propagator $S(q)$, which, dynamically dressed through its SD-equation, contains the momentum-dependent functions $A(q^2)$ and $B(q^2)$. The bare vertex γ^μ obviously violates the vector WTI, implying the non-conservation of the electromagnetic vector current and charge. Solving the pertinent SD equation for the dressed quark–photon–quark ($qq\gamma$) vertex Γ^μ is still an unsolved problem, and using the realistic Ansätze for Γ^μ is presently the only practical way to satisfy the WTI. Following Refs. 6, 27, 5 and 8 (for example), we can choose the Ball–Chiu (BC)

[28] vertex; *i.e.*, $\Gamma^\mu = \Gamma^\mu_{BC}$,

$$\Gamma^\mu_{BC}(q',q) = A_+(q'^2,q^2)\frac{\gamma^\mu}{2} + \frac{(q'+q)^\mu}{(q'^2-q^2)}\{A_-(q'^2,q^2)\frac{(\not{q}'+\not{q})}{2} - B_-(q'^2,q^2)\}\ , \quad (6)$$

where $H_\pm(q'^2,q^2) \equiv [H(q'^2) \pm H(q^2)]$, for $H = A$ or B. This particular solution of the vector WTI reduces to the bare vertex in the free-field limit as must be in perturbation theory, has the same transformation properties under Lorentz transformations and charge conjugation as the bare vertex, and has no kinematic singularities. It does *not* introduce any new parameters as it is completely determined by the dressed quark propagator $S(q)$.

Another WTI-preserving choice for Γ^μ can be a vertex of the Curtis–Pennington (CP) type, *i.e.*, $\Gamma^\mu \equiv \Gamma^\mu_{BC} + \Delta\Gamma^\mu$ where the the transverse addition $\Delta\Gamma^\mu$ is of the type [29]

$$\Delta\Gamma^\mu(q',q) = \frac{\gamma^\mu(q'^2-q^2) - (q'+q)^\mu(\not{q}'-\not{q})}{2d(q',q)}A_-(q'^2,q^2)\,. \quad (7)$$

Two especially suitable *Ansätze* for the dynamical function $d(q',q)$, ensuring multiplicative renormalizability of fermion SDE beyond the ladder approximation in QED_4, are

$$d_\pm(q',q) = \frac{1}{q'^2+q^2}\left\{(q'^2 \pm q^2)^2 + \left[\frac{B^2(q'^2)}{A^2(q'^2)} + \frac{B^2(q^2)}{A^2(q^2)}\right]^2\right\}\ . \quad (8)$$

The original CP *Ansatz* $\Gamma^\mu \equiv \Gamma^\mu_{CP}$ employed $d(q',q) = d_-(q',q)$ [29]. We will use it in analytic calculations of $T(-Q^2,0)$, which are possible for $Q^2 = 0$ and $Q^2 \to \infty$. However, in the numerical calculations, which are necessary for finite values of $Q^2 \neq 0$, we prefer to restrict ourselves (besides the minimal BC vertex) to the *modified* CP (mCP) vertex, Γ^μ_{mCP}, resulting from the choice $d = d_+$ in Eq. (7). Namely, as pointed out in Ref. 21, the numerical calculation of $T(-Q^2,0)$ employing Γ^μ_{mCP} vertices is free from certain numerical difficulties arising, in this application, from the CP denominator function $d_-(q',q)$.

In contrast to the BC one, the mCP vertex is also consistent with multiplicative renormalizability, like the original CP vertex. In the present context, the important *qualitative* difference between the BC-vertex on one side, and the CP vertex as well as the modified, mCP vertex on the other side, will be that $\Gamma^\mu_{BC}(q',q) \to \gamma^\mu$ when *both* $q'^2, q^2 \to \pm\infty$, whereas $\Gamma^\mu_{CP}(q',q) \to \gamma^\mu$ and $\Gamma^\mu_{mCP}(q',q) \to \gamma^\mu$ as soon as *one* of the squared momenta tends to infinity. This turned out [21] to lead to the same coefficient of the $Q^2 \to \infty$ behaviour (4) for the CP vertices and mCP vertices, namely $\mathcal{J} = 4/3$, but a larger one for the BC-vertices.

We have checked that the $Q^2 = 0$ case, *i.e.*, the $\pi^0 \to \gamma\gamma$ amplitude (1), is reproduced analytically employing the CP vertices and mCP vertices in the same way as when the BC vertices were employed in earlier applications, *e.g.* in Refs. 5, 6, 9 and 10.

In the case of π^0, GIA yields (e.g., see Eq. (24) in Ref. 10) the amplitude $T^{\mu\nu}_{\pi^0}(k,k')$:

$$T^{\mu\nu}_{\pi^0}(k,k') = -N_c \frac{1}{3\sqrt{2}} \int \frac{\mathrm{d}^4 q}{(2\pi)^4} \mathrm{Tr}\{\Gamma^\mu(q-\frac{p}{2}, k+q-\frac{p}{2}) S(k+q-\frac{p}{2})$$

$$\times \Gamma^\nu(k+q-\frac{p}{2}, q+\frac{p}{2}) \chi(q,p)\} + (k \leftrightarrow k', \mu \leftrightarrow \nu). \qquad (9)$$

Here, χ is the BS amplitude of both $u\bar{u}$ and $d\bar{d}$ pseudoscalar bound states: $\chi \equiv \chi_{u\bar{u}} = \chi_{d\bar{d}}$ thanks to the isospin symmetry assumed here. This symmetry likewise enables us to continue suppressing flavour labels also on the quark propagators S and $qq\gamma$ vertices Γ^μ. We follow the conventions of Ref. 10, including those for the flavour factors and flavour matrices λ^a. Then, $\chi_{\pi^0}(q,p) \equiv \chi(q,p)\,\lambda^3/\sqrt{2}$, so that the prefactor $1/3\sqrt{2}$ in Eq. (9) is just the flavour trace $\mathrm{tr}(\mathcal{Q}^2\lambda^3/\sqrt{2})$ where $\mathcal{Q} = \lambda^3/2 + \lambda^8/2\sqrt{3} = diag(+2/3, -1/3, -1/3)$ is the quark charge matrix.

3. *Our results and comparison with others*

Already in Ref. 9 (where only the BC vertex was employed), the transition form factor $T_{\pi^0}(-Q^2, 0)$ was numerically evaluated (for $0 < Q^2 < 2.8$ GeV^2 only) employing - for the pion only - the soft and chiral limit (3).

In the subsequent work [21], we went beyond this approximation, using our complete solution for the BS vertex $\Gamma_{\pi^0}(q,p)$, *viz.* the BS amplitude $\chi_{\pi^0}(q,p)$, given by the decomposition into 4 scalar functions multiplying independent spinor structures. We calculated the transition form factor not only for the BC vertex, but also the mCP vertex. The approximation we kept in Ref. 21 (and which we still keep in the present paper), is discarding the second and higher derivatives in the momentum expansions of the SD solutions $A(q^2)$ and $B(q^2)$ and BS solutions $\chi(q,p)$. In Ref. 21, $T_{\pi^0}(-Q^2,0)$ was evaluated up to $Q^2 \approx 8$ GeV^2, which is roughly the limit of the presently accessible transferred momenta. In this paper, we evaluate the transition form factor up to 36 GeV^2. We present curves for $Q^2 T_{\pi^0}(-Q^2,0)$ evaluated in various ways first in Fig. 1, depicting their evolution all the way to 36 GeV^2. This squeezes the presently existing experimental points into the first quarter of the scale; however, the issue of comparing and improving the agreement with the data at the accessible momenta will be returned to later, and now we want first to illustrate how various theoretical transition form factors at finite Q^2 connect to the asymptotic behaviour.

In Fig. 1, the solid line is our prediction for $Q^2 T_{\pi^0}(-Q^2,0)$ evaluated with the BC vertex. It reaches the asymptotic behaviour faster than other curves. Already after $Q^2 \approx 4$ GeV^2, the tiny changes cannot be observed in the solid line, but only in the corresponding numerical data, as the asymptotic value is approached from below. For comparison, the dash-dotted line gives the results obtained (also with the BC vertex) in the approximation (3) of soft and chiral limit as explained above. At

$Q^2 \approx 4$ GeV^2, where the $Q^2 T_{\pi^0}(-Q^2, 0)$ from the full calculation already practically reaches the asymptotic limit, the difference between it and $Q^2 T^{soft}_{\pi^0}(-Q^2, 0)$ from the approximation (3), is somewhat above 10%. This difference gets bigger as Q^2 grows, and asymptotically it reaches some 22% of the limit value of $Q^2 T_{\pi^0}(-Q^2, 0)$. However, this still means that the effect of the soft limit approximation on the transition form factor is much less than on the charge form factor. Namely, Maris and Roberts [30] pointed out that omitting the pseudovector components of the pion lead even to the wrong asymptotic behaviour, as $1/Q^4$ instead of $1/Q^2$, in the case of the charge form factor of the pion. In the present case of the transition form factor, the correct $1/Q^2$ leading behaviour is nevertheless obtained not only for the results of the full calculation, but also in the soft limit approximation (3). It is just that the coefficient of $1/Q^2$ is underestimated with respect to the full calculation.

The dashed line was obtained in the same way as the solid line, but employing the mCP vertex. Even at $Q^2 = 36$ GeV^2, the asymptotic behaviour is obviously not yet reached in the case of the mCP vertex. However, later we will comment on how Ref. 21 showed analytically that the behaviour given by Eq. (4) must be reached at some point, although at much higher values of Q^2 when the mCP vertex is used.

How do our transition form factors agree with other theoretical approaches? The vector–meson dominance (VMD) model and the QCD sum rule approach [18] give the transition form factor which is some 10% below our "BC" $T_{\pi^0}(-Q^2, 0)$ for the *presently* largest accessible values of Q^2, *i.e.*, around 8 GeV^2. Therefore, in that region, our BC-results are between the uppermost line in Fig. 1 (the dotted constant line at $2f_\pi$) denoting the asymptotic pQCD [15] version ($\mathcal{J} = 2$) of Eq. (4), and the results of VMD (e.g., see Ref. 14), the recent pQCD calculation by Ref. 31 as well as the QCD sum rule results of Radyushkin and Ruskov [18]. $Q^2 T_{\pi^0}(-Q^2, 0)$ of VMD and pQCD rise with Q^2, albeit with different rates, while that from the QCD sum rules of Ref. 18 starts almost imperceptibly falling after $Q^2 \approx 7$ GeV^2.

The large-Q^2 leading power-law behaviour (4) was first derived from the parton picture in the infinite momentum frame – e.g., see Ref. 15. In this and other similar pQCD approaches, the precise value of the coefficient of the leading $1/Q^2$ term depends on the pion distribution amplitude $\varphi_\pi(x)$ which should contain the necessary nonperturbative information about the probability that a partonic quark carries the fraction x of the total longitudinal momentum. *E.g.*, the well-known example of a "broad" distribution $\varphi^{CZ}_\pi(x) = f_\pi 5\sqrt{3}x(1-x)(1-2x)^2$ (proposed by Chernyak and Zhitnitsky [19] motivated by sum-rule considerations) leads to $\mathcal{J} = 10/3$, but it is too large in the light of the latest data [12]. In contrast, the asymptotic distribution $\varphi^A_\pi(x) = f_\pi\sqrt{3}x(1-x)$ (depicted by dotted line in Fig. 2 and favoured by Lepage and Brodsky [15]) yields $\mathcal{J} = 2$, resulting in the constant dotted line crossing the upper error bar of the presently highest-Q^2 data point in Fig. 1.

In the *strict* $\ln(Q^2) \to \infty$ limit, every distribution amplitude must evolve into the asymptotic one, $\varphi_\pi(x) \to \varphi^A_\pi(x)$, if the effects of the pQCD evolution are taken into account [15]. However, even at Q^2-values larger than the presently accessible

ones, other effects may still be more important than the effects of the pQCD evolution. This is the reason why other approaches and other forms of $\varphi_\pi(x)$ should be considered even when they do not incorporate the pQCD evolution. This is in line with Radyushkin and Ruskov's (Ref. 18 and references therein) pointing out desirability of having direct calculations of $T_{\pi^0}(-Q^2,0)$ without *a priori* assumptions about the pion distribution amplitude φ_π. One can then consider the opposite procedure from the one which is standard in pQCD: from such direct calculations of $T_{\pi^0}(-Q^2,0)$, one can draw conclusions about the distribution amplitude φ_π.

The form

$$\varphi_\pi(x) = \frac{f_\pi}{2\sqrt{3}} \frac{\Gamma(2\zeta+2)}{[\Gamma(\zeta+1)]^2}\, x^\zeta\, (1-x)^\zeta\,, \quad \zeta > 0\,, \tag{10}$$

is suitable for representing various distribution amplitudes because it is relatively general [15]: $\zeta > 1$ yields the distributions that are "peaked" or "narrowed" with respect to the asymptotic one ($\zeta = 1$), whereas $\zeta < 1$ gives the "broadened"

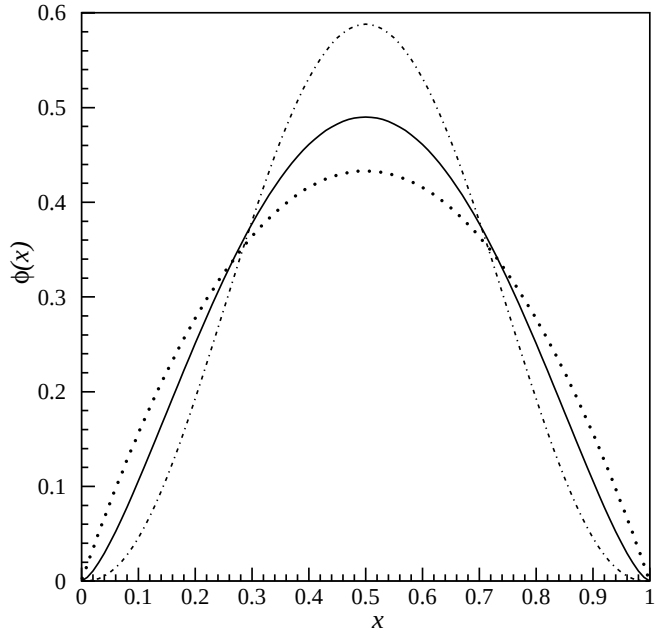

Fig. 2. The pion distribution amplitudes (10) are depicted in the dimensionless version $\phi(x) \equiv \varphi_\pi(x)/f_\pi$ for the three values of ζ pertinent to the discussion in this paper. $\zeta = 1$ yields the asymptotic distribution amplitude (the dotted curve), $\zeta = 1.5$ pertains to the pion distribution amplitude depicted by the solid curve and corresponds to the large-Q^2 values of our $T_{\pi^0}(-Q^2,0)$ evaluated with the BC $qq\gamma$ vertex. $\zeta = 2.5$ corresponds to the transition form factors predicted by Refs. 31 and 18 for the largest Q^2-values ($Q^2 \approx 8$ GeV^2) at which $T_{\pi^0}(-Q^2,0)$ has been measured so far.

distributions which, however, now seems to be ruled out for the same reason as $\varphi_\pi^{CZ}(x)$ quoted above, since $\mathcal{J} > 2$ is ruled out empirically by CLEO [12]. Namely, it is easy to see that Eq. (10) implies $\zeta = 2/(3\mathcal{J} - 4)$.

In Fig. 2, we plot the distribution amplitudes of the form (10) for the three cases that are the most interesting for the present discussion. As seen below, these cases correspond to the ζ-values equal to 1 (dotted line), 1.5 (solid line), and 2.5 (dash-dotted line).

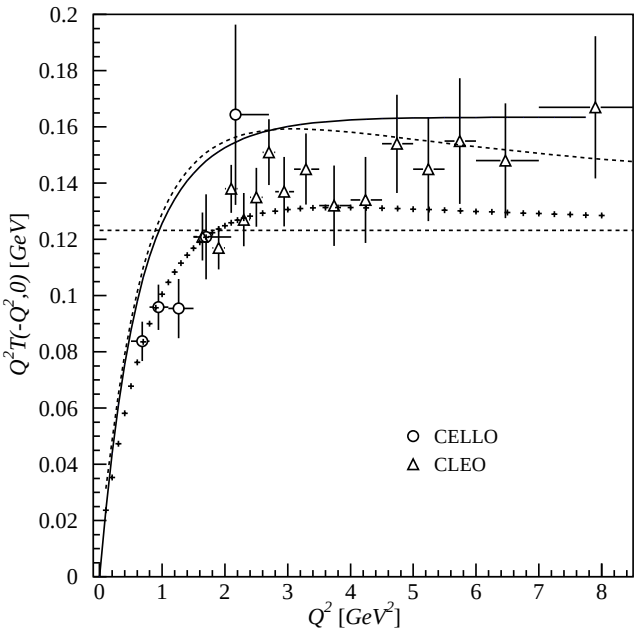

Fig. 3. The comparison of our results for the pion transition form factor (times Q^2) with the CELLO (circles) and CLEO (triangles) data. Our results for $Q^2T_{\pi^0}(-Q^2,0)$ are depicted by the solid line for the case of the BC vertex, and by the dashed line for the case of the mCP vertex. This latter one gets lower beyond $Q^2 \approx 2.5$ GeV^2 and does not yet saturate at the presently accessible momenta although approaches asymptotically $Q^2T_{\pi^0}(-Q^2,0) \to 4f_\pi/3$ for much higher Q^2. (This limit is denoted by the dashed straight line.) The little crosses denote (for both BC and mCP $qq\gamma$ vertices) our $Q^2T_{\pi^0}(-Q^2,0)$ when we enforce $A(q^2) \equiv 1$ by hand.

At the highest presently accessible momenta, the asymptotic prediction ($\mathcal{J} = 2$) is lowered by some 20% by the lowest order QCD radiative corrections [31], amounting to $\mathcal{J} \approx 1.6$, which fits the CLEO data well. Of course, these QCD corrections mean that $Q^2T_{\pi^0}(-Q^2,0)$ is not strictly constant, but according to Ref. 31, it rises towards $2f_\pi$ so slowly that we can take it constant in practice. [Eqs. (19) and (18) from Ref. 31 lead to the line of empty squares in Fig. 1, that is, to $Q^2T_{\pi^0}(-Q^2,0)$ which grows just 4% from $Q^2 = 9$ GeV^2 to $Q^2 = 36$ GeV^2 when the

number of relevant flavours is set to $N_f = 5$. The full calculation [31], which employs the momentum-dependent N_f [32], seems to give even slower variation of $Q^2 T_{\pi^0}$ – see their Fig. 2.] Similarly slow variation results from the sum-rule approach of Radyushkin and Ruskov [18], which yields the transition form factor which is, on the interval from 3 to 8 GeV^2, quite close to those of the pQCD approach of Brodsky *et al.* [31]. The sum-rule [18] $Q^2 T_{\pi^0}(-Q^2, 0)$ starts actually *falling* after $Q^2 \sim 7$ GeV^2, but so slowly that Eq. (4) with the constant $\mathcal{J} \approx 1.6$ represents it accurately at the presently accessible values of Q^2. This, just like roughly the same $\mathcal{J}$ associated to Ref. 31, corresponds to a rather narrow distribution (10) with $\zeta \approx 2.5$, depicted by the dash-dotted line in Fig. 3.

The leading large-Q^2 behaviour as in Eq. (4), was obtained also by Manohar [20] using the operator product expansion (OPE). According to his OPE calculation, the coefficient in Eq. (4) giving the leading term is $\mathcal{J} = 4/3$, which is below our large-Q^2 $T_{\pi^0}(-Q^2, 0)$ by $\approx 20\%$ when we use the BC vertex, but exactly coincides with the $Q^2 \to \infty$ limit obtained when we use the CP or the mCP vertex – see Ref. 21 and comments below. The coefficient $\mathcal{J} = 4/3$ is the lowest one still consistent with the form (10) because it corresponds to $\zeta = \infty$. The pion distribution amplitude (10) then becomes infinitely peaked delta function: $\varphi_\pi(x) = (f_\pi/2\sqrt{3})\,\delta(x - 1/2)$.

For $Q^2 > 4$ GeV^2, our "BC" $T_{\pi^0}(-Q^2, 0)$ also behaves in excellent approximation as (4), with $\mathcal{J} \approx 1.78$. This would in the pQCD factorization approach correspond to $\varphi_\pi(x)$ (10) with $\zeta \approx 1.5$. On the other hand, our "mCP" $T_{\pi^0}(-Q^2, 0)$ falls off faster than $1/Q^2$ for even the largest of the Q^2 values depicted in Fig. 2. However, it does not fall off much faster, as our "mCP" $Q^2 T_{\pi^0}(-Q^2, 0)$ at $Q^2 = 18$ GeV^2 is only 6%, and at the huge $Q^2 = 36$ GeV^2 is only 10% smaller than at $Q^2 = 9$ GeV^2 (roughly the highest presently accessible Q^2). Moreover, Ref. 21 showed analytically that, generally, the $1/Q^2$-behaviour of Eq. (4) is at some point reached in our approach, although Fig. 1 shows that for the mCP $qq\gamma$ vertices this can happen only at significantly higher Q^2 than it happens for the BC $qq\gamma$ vertices.

4. *Discussion, comments and conclusions*

The most important novelty in Ref. 21 is its result on the large-Q^2 asymptotic behaviour. Namely, it implies that the modern version of the constituent quark model which is given by the coupled SD-BS approach, provides from $Q^2 = 0$ to $Q^2 \to \infty$ the description for $\gamma\gamma^\star \to \pi^0$ which is – independently of model details – consistent not only with the Abelian axial anomaly but also with the QCD predictions (4) for the leading large-Q^2 behaviour. In the SD-BS approach, f_π is a quantity calculable through the straightforward application of the Mandelstam-formalism expression

$$p_\mu f_\pi = \mathrm{i} \frac{N_c}{\sqrt{2}} \int \frac{\mathrm{d}^4 q}{(2\pi)^4} \mathrm{Tr}[\chi(q,p)\gamma_\mu\gamma_5]\,. \tag{11}$$

The model dependence is present in the (successfully reproduced [7,9,10,3]) *value* of f_π, but the derivation [21] of the asymptotic *forms* (4) and (15) below, is model-

independent. They do not depend on what are the bound-state solutions, just like the chiral-limit axial-anomaly amplitude (1) doesn't.

Of special importance is also that the derivation in Ref. 21 of the asymptotic large-Q^2 forms (4) and (15) below, applies to both Minkowski and Euclidean space.

Our result [21] on the asymptotic behaviour of $T_{\pi^0}(-Q^2,0)$ subsequently received further support from Roberts [33], who generalized its derivation by taking into account renormalization explicitly. His derivation shows that the asymptotics of Ref. 21 obtained using the CP or mCP vertex, namely $\mathcal{J}=4/3$, must be precisely reproduced for any $qq\gamma$ vertex which is (like the CP or mCP ones) consistent with multiplicative renormalizability.

It is interesting that the asymptotic behaviour for large negative $k^2=-Q^2$ predicted [21] for the bare $qq\gamma$ vertex and, e.g., the dressed CP and mCP ones, is in exact agreement with the leading term predicted by Manohar using OPE [20]. In this paper, we shed some light on this connection by providing the following alternative derivation of the asymptotic behaviour: consider $TJ^\mu_a(x)J^\nu_b(x)$, the T-product of two quark vector currents $J^\mu_a(x)=\bar\psi(x)\gamma^\mu(\lambda^a/2)\psi(x)$, along the lines of Ref. 34 (Ch. 18 on OPE), but evaluated between the pion state and the vacuum. We substitute for the quark propagator its leading light cone $[(x-y)^2\to 0]$ behaviour

$$S(x-y)\approx\frac{2(x-y)\cdot\gamma}{(2\pi)^2[(x-y)^2-\mathrm{i}\epsilon]^2}\,, \tag{12}$$

and utilize $\gamma^\mu\gamma^\lambda\gamma^\nu=\mathcal{S}^{\mu\lambda\nu\sigma}\gamma_\sigma-i\varepsilon^{\mu\lambda\nu\sigma}\gamma_\sigma\gamma_5$ similarly as in the derivation of the large Q^2-behaviour in Ref. 21. The term which contains the symmetric tensor $\mathcal{S}^{\mu\lambda\nu\sigma}=g^{\mu\lambda}g^{\nu\sigma}+g^{\mu\sigma}g^{\lambda\nu}+g^{\mu\nu}g^{\lambda\sigma}$, is readily seen not to contribute to the $\pi^0\gamma\gamma^\star$ vertex. On the other hand, in the term containing the antisymmetric Levi-Civita tensor $\varepsilon^{\mu\lambda\nu\sigma}$ and γ_5, one finds – in the lowest order of the $(x-y)$-expansion – the pion-to-vacuum matrix element of the axial current,

$$\langle 0|\bar\psi(0)\gamma_\mu\gamma_5\mathcal{Q}^2\psi(0)|\pi^3(p)\rangle=\frac{1}{3}\langle 0|\bar\psi(0)\gamma_\mu\gamma_5\frac{\lambda^3}{2}\psi(0)|\pi^3(p)\rangle=\frac{1}{3}\,\mathrm{i}\,f_\pi\,p_\mu\,, \tag{13}$$

defining the pion decay constant f_π. The coordinate-space integration is reduced to

$$\int\mathrm{d}^4x\,e^{\mathrm{i}k\cdot x}\frac{x_\lambda}{(x^2-\mathrm{i}\epsilon)^2}=2\pi^2\,\frac{k_\lambda}{k^2+\mathrm{i}\epsilon}\,. \tag{14}$$

Putting all this together reveals that the lowest-order result in the $(x-y)$-expansion is just Eq. (4) with $\mathcal{J}$ being precisely 4/3.

We thus in another way recover the result of OPE [20], of Ref. 21 for the cases employing any vertex (e.g., CP or mCP) which tends to the bare one (γ_μ) as soon as one of its legs is hard, and of subsequent generalization [33] thereof for any $qq\gamma$ vertices consistent with the multiplicative renormalization. However, this asymptotic behaviour $Q^2T_{\pi^0}(-Q^2,0)=(4/3)f_\pi$ lies some 20% below the central values of the largest-Q^2 CLEO data, and is more than one standard deviation away

from them. Nevertheless, Manohar [20] pointed out that his OPE approach also indicates the existence of potentially large corrections to his leading term.

Let us now return to the BC vertex, which has been the most commonly used dressed $qq\gamma$ vertex in the phenomenological SD-BS calculations so far. In conjunction with our SD-BS solutions, the usage of the BC vertex raises the asymptotic coefficient $\mathcal{J}$ of Eq. (4) from 4/3 resulting from the usage of the bare, CP and mCP vertices, to $\mathcal{J} \approx 1.78$. The reason for this enhancement is that the BC vertex does not reduce to the bare vertex γ^μ if the large momenta flow through just one, and not both, of its fermion legs. (Also note that the BC vertex is not consistent with multiplicative renormalizability [35,29], so that the arguments of Ref. 33 are not applicable to it.) It was shown in Ref. 21 that when the BC vertex is used in our approach, the predicted asymptotic behaviour is

$$T_{\pi^0}(-Q^2,0) \to \frac{4}{3}\frac{\widetilde{f}_\pi}{Q^2} \tag{15}$$

where $\widetilde{f}_\pi$ is given by the same expression (11) as f_π, except that the integrand is modified by the factor $[1+A(q^2)]^2/4$. In the special case of the solutions we use, the slow and moderate variation of $A(q^2)$, as well as its shape (see Fig. 3 in Ref. 3) permits the approximate factorization

$$\widetilde{f}_\pi \approx f_\pi \frac{[1+A(0)]^2}{4}. \tag{16}$$

This last approximation (a rather rough one) would imply $\mathcal{J} \approx 1.69$, *i.e.*, $Q^2 T_{\pi^0}(-Q^2,0) \to 0.157$ GeV. The more accurate Eq. (15) gives $Q^2 T_{\pi^0}(-Q^2,0) \to 0.168$ GeV. This is practically indistinguishable from the asymptotics indicated by our full numerical calculation of the transition form factor, which reached $Q^2 T_{\pi^0}(-Q^2,0) \approx 0.165$ GeV at the largest numerically studied Q^2. It is of special importance that analytically obtained large-Q^2 asymptotics (15), the derivation of which is valid in both Minkowski and Euclidean space, makes this smooth and accurate contact between our large-Q^2 numerical results calculated with the Euclidean solutions of the chosen model [7]. The excellent agreement between the analytical and numerical results confirms the accuracy of our numerical methods and procedures (employing the Euclidean bound-state solutions [7]) used in this and earlier papers [9,10,3].

Another case of this agreement between the numerical results and the analytical considerations is provided by $Q^2 T_{\pi^0}(-Q^2,0)$ found in the soft and chiral limit approximation (3). Therefore, let us for a moment consider again this approximation, although we surpassed it already in Ref. 21. (As a bonus, we also gain understanding of some subtle aspects in its previous applications.) In Fig. 1, the results of the numerical calculation in that approximation, and with the BC vertex (6), are depicted by the dash-dotted line, which practically reaches (from above) the asymptotic behaviour, although not as fast as the results without that approximation, depicted by the solid line. We now note that in the approximation (3),

the asymptotic behaviour (15) should be realized with f_π and $\widetilde{f}_\pi$ calculated in the *same* approximation. We will denote them by f_π^{gPS} and $\widetilde{f}_\pi^{gPS}$, where gPS is short for "generalized Pagels-Stokar". Namely, it turns out [23] that the soft limit approximation (3), when applied to f_π, is the same as the widely used Pagels-Stokar approximation [36] *except* that they work with the restriction $A(q^2) \equiv 1$ – unlike the present approach. Since we find $\widetilde{f}_\pi^{gPS} = 109.2$ MeV, it appears that our dash-dotted curve should approach $Q^2 T_{\pi^0}^{soft}(-Q^2, 0) \to (4/3)\widetilde{f}_\pi^{gPS} = 0.146$ GeV. In fact, at $Q^2 = 36$ GeV^2, $Q^2 T_{\pi^0}^{soft}(-Q^2, 0) \approx 0.136$ GeV. To understand what forced the dash-dotted curve below, let us remember that the factor $1/f_\pi$ appears in Eq. (3) because in the chiral limit it turns out that the pion decay constant f_π is precisely equal to the the normalization of the BS vertex $\Gamma_\pi(p, q)$ [37]. In Ref. 9, the transition form factor was thus found using in Eq. (3) our chiral-limit value of the pion decay constant, $f_\pi = f_\pi^0 = 89.8$ MeV, and to make contact with that reference we have evaluated in this paper the dash-dotted curve in the same way. However, from what has just been explained, it follows that when we use not only the chiral, but also the soft limit (3), the normalization of the BS vertex is given by the pion decay constant calculated in the same approximation, $f_\pi = f_\pi^{gPS}$, which in our adopted model has the value of 80.8 MeV. The transition form factor of Ref. 9 was thus suppressed by the factor f_π^{gPS}/f_π^0; for the same reason, the dash-dotted line in the present Fig. 1 approaches from above $(4/3)\widetilde{f}_\pi^{gPS}(f_\pi^{gPS}/f_\pi^0) \approx 0.131$ GeV as the limiting value, so everything tallies.

In the case of the BC vertex, the "soft" leg adjacent to the pion BS-amplitude always contributes $A(q^2)$, which enhances the asymptotic value of $Q^2 T_{\pi^0}(-Q^2, 0)$. This is not so for vertices such as the CP or mCP ones. Since they tend to the bare vertex as soon as the high momentum flows through one of their legs, f_π does *not* get replaced by $\widetilde{f}_\pi$, and the "bare" result, Eq. (4) with $\mathcal{J} = 4/3$, continues to hold for $Q^2 \to \infty$ when such vertices are used.

Of course, the usage of the mCP vertex instead of the bare γ^μ makes a considerable difference for the finite Q^2. Let us therefore now focus our attention to Fig. 3, which shows $Q^2 T_{\pi^0}(-Q^2, 0)$ found in our approach for both the BC-case (solid curve) and the mCP-case (dashed curve) for the interval of the transferred momenta between the presently highest accessible Q^2 and $Q^2 = 0$.

At $Q^2 = 0$, both BC and mCP vertices give the same amplitude (1) for $\pi^0 \to \gamma\gamma$ in the chiral limit. With growing Q^2, the BC and mCP curves in Fig. 3 must nevertheless ultimately separate because of the difference $(4/3)(\widetilde{f}_\pi - f_\pi)$ of their large-Q^2 limiting values. At the highest presently accessible momenta, $Q^2 \approx 8$ GeV^2, they differ by 9%, but as we go down in Q^2, we see that already for $Q^2 \lesssim 4$ GeV^2, they practically coincide. This insensitivity on the choice of the WTI-preserving $qq\gamma$-vertex is very indicative. Namely, the true solution for the $\Gamma^\mu(p, p')$ vertex, the one which we try to imitate by the BC and mCP vertex *Ansätze*, is – for $Q^2 \lesssim 4$ GeV^2 – unlikely to give $Q^2 T_{\pi^0}(-Q^2, 0)$ significantly different from the BC and mCP vertices, since at $Q^2 = 0$ the transition amplitude must (in the chiral limit) again be (1), and at larger Q^2 the difference should not be larger than that resulting

from the BC and mCP vertices, as they lead to so very different $Q^2 T_{\pi^0}(-Q^2, 0)$ as $Q^2 \to \infty$. (One should also keep in mind that the multiplication by Q^2 serves only for exposing the asymptotics more clearly, and that the difference is even smaller for $T_{\pi^0}(-Q^2, 0)$ proper, which must in every case decrease as $1/Q^2$.) The weak sensitivity (at least for not too large Q^2) on the WTI-preserving *Ansatz* for $\Gamma^\mu(p, p')$ means that high-precision measurements of $T_{\pi^0}(-Q^2, 0)$ will test unambiguously (and possibly give a hint on how to improve) the SD and BS model solutions which have so far been successful in fitting the low-energy hadron properties such as the meson spectrum. For example, our model choice [7] obviously (for both BC and mCP vertices) slightly overestimates $T_{\pi^0}(-Q^2, 0)$ in the region $Q^2 \lesssim 4$ GeV^2.

We point out that out of various SDE and BSE solutions in the SD-BS approach, once that f_π has been correctly reproduced by χ [see Eq. (11)], the transition form factor is most sensitive on $A(q^2)$, or, more precisely, on its values at small and intermediate momenta $-q^2$, where $A(q^2)$ is still appreciably different from 1. Eqs. (15)-(16) already explained how $A(q^2)$ drives $Q^2 T_{\pi^0}(-Q^2, 0)$ upwards through $\widetilde{f_\pi}$ for large Q^2 in the case of the BC vertex.

To illustrate what happens at $Q^2 \lesssim 8$ GeV^2 when the $A(q^2)$-profile is decreased, let us enforce by hand the extreme, artificial case $A(q^2) \equiv 1$. (To avoid confusion, we stress it is for illustrative purposes only, as we cannot have such a SD-solution in the adopted approach of Refs. 23, 24 and 7.) This leads to the curve traced on Fig. 3 by small crosses, pertaining to the usage of both BC and mCP vertices (as well as the CP ones), since $A(q^2) \equiv 1$ makes $\Gamma^\mu_{mCP} \to \Gamma^\mu_{BC}$. This curve illustrates how the heights of the curves depicting $Q^2 T_{\pi^0}(-Q^2, 0)$ depend on how much the $A(q^2)$-profile exceeds 1. Obviously, for both the solid curve and the dashed one, the agreement with experiment would be improved by lowering them somewhat (at least in the momentum region $Q^2 \lesssim 4$ GeV), which could be achieved by modifying the model [7] and/or its parameters so that such a new solution for $A(q^2)$ is somewhat lowered towards its asymptotic value $A(q^2 \to \infty) \to 1$. (Of course, in order to be significant, this must not be a specialized re-fitting aimed *only* at $A(q^2)$. Lowering of $A(q^2)$ must be a result of a broad fit to many meson properties, comparable to the original fit [7]. This, however, is beyond the scope of this paper.)

By the same token, high precision measurements of $T_{\pi^0}(-Q^2, 0)$ (such as those planned at Jefferson Lab [13]) can be especially helpful in obtaining information on $A(q^2)$ empirically. First note that Fig. 3 reveals that in the region around $Q^2 \approx 4$ GeV^2 we are already in the regime where the dependence on the BS-amplitude χ is lumped into f_π. Therefore, high-precision measurements of $T_{\pi^0}(-Q^2, 0)$ in the region close to the asymptotic regime will give information on the integrated strength of $A(q^2)$ although not on $A(q^2)$ itself. However, since it is known that the form of that function must be a rather smooth transition (e.g., see Ref. 3) from $A(q^2) > 1$ for Q^2 near 0, to $A(q^2) \to 1$ in the Q^2-domain where QCD is perturbative, such measurements [13] would give a useful hint even about $A(q^2)$ itself – namely about what solutions for $A(q^2)$ one may have in sensible descriptions of dynamically dressed quarks and their bound states.

Acknowledgements

The authors acknowledge the support of the Croatian Ministry of Science Technology to the conference "Nuclear and Particle Physics with CEBAF at Jefferson Lab", Dubrovnik, Croatia, November 3-10, 1998.

References

1) C. D. Roberts, *Nonperturbative QCD with modern tools*, nucl-th/9807026;
2) C. D. Roberts and A. G. Williams, Prog. Part. Nucl. Phys. **33** (1994) 477;
3) D. Kekez, B. Bistrović and D. Klabučar, Int. J. Mod. Phys. A **14** (1999) 161;
4) M. Bando, M. Harada and T. Kugo, Prog. Theor. Phys. **91** (1994) 927;
5) C. D. Roberts, Nucl. Phys. A **605** (1996) 475;
6) M. R. Frank, K. L. Mitchell, C. D. Roberts and P. C. Tandy, Phys. Lett. B **359** (1995) 17;
7) P. Jain and H. J. Munczek, Phys. Rev. D **48** (1993) 5403;
8) R. Alkofer and C. D. Roberts, Phys. Lett. B **369** (1996) 101;
9) D. Kekez and D. Klabučar, Phys. Lett. B **387** (1996) 14;
10) D. Klabučar and D. Kekez, Phys. Rev. D **58** (1998) 096003;
11) H.-J. Behrend et al., (CELLO Collaboration), Z. Phys. C **49** (1991) 401;
12) J. Gronberg et al., (CLEO collaboration), Phys. Rev. D **57** (1998) 33;
13) CEBAF Letter of Intent # LOI–94/005. co-spokesmen: A. Afanasev, J. Gomez and S. Nanda; A. Afanasev, hep-ph/9608305;
14) M. Hayakawa and T. Kinoshita, Phys. Rev. D **57** (1998) 465;
15) G. P. Lepage and S. J. Brodsky, Phys. Rev. D **22** (1980) 2157; S. J. Brodsky and G. P. Lepage, *ibid.* **24** (1981) 1808;
16) R. Jakob et al., J. Phys. G **22** (1996) 45; P. Kroll and M. Raulfs, Phys. Lett. B **387** (1996) 848; F.-G. Cao, T. Huang and B. Q. Ma, Phys. Rev. D **53** (1996) 6582;
17) I. V. Musatov and A. V. Radyushkin, Phys. Rev. D **56** (1997) 2713;
18) A. V. Radyushkin and R. T. Ruskov, Nucl. Phys. B **481** (1996) 625; *The asymptotics of the transition form factor* $\gamma\gamma^\star \to \pi^0$ *and QCD sum rules*, hep-ph/9706518;
19) V. L. Chernyak and A. R. Zhitnitsky, Phys. Rep. **112** (1984) 173, and references therein.
20) A. Manohar, Phys. Lett. **B244** (1990) 101;
21) D. Kekez and D. Klabučar, Phys. Letters B **457** (1999) 359; $\gamma^\star\gamma \to \pi^0$ *transition and asymptotics of* $\gamma^\star\gamma$ *and* $\gamma^\star\gamma^\star$ *transitions of other unflavoured pseudoscalar mesons*, hep-ph/9812495;
22) P. Maris and C. D. Roberts, Phys. Rev. C **56** (1997) 3369;
23) P. Jain and H. J. Munczek, Phys. Rev. D **44** (1991) 1873;
24) H. J. Munczek and P. Jain, Phys. Rev. D **46** (1992) 438;
25) A. Bender, C. D. Roberts, and L. V. Smekal, Phys. Lett. B **380** (1996) 7;

26) V. A. Miransky, *Dynamical symmetry breaking in quantum field theories*, World Scientific Publishing Co., Singapore (1993), ISBN 981-02-1558-4);

27) C. J. Burden, C. D. Roberts and M. J. Thompson, Phys. Lett. B **371** (1996) 163;

28) J. S. Ball and T.-W. Chiu, Phys. Rev. D **22** (1980) 2542;

29) D. C. Curtis and M. R. Pennington, Phys. Rev. D **42** (1990) 4165;

30) P. Maris and C. D. Roberts, Phys. Rev. **C58** (1998) 3659;

31) S. J. Brodsky, C.-R. Ji, A. Pang and D. G. Robertson, Phys. Rev. D **57** (1998) 245;

32) D. V. Shirkov and S. V. Mikhailov, Z. Phys. C **63** (1994) 463;

33) C. D. Roberts, *Dyson Schwinger equations: connecting small and large length-scales*, nucl-th/9901091; submitted to Fizika B (Zagreb) **8** (1999) XXXXX;

34) F. J. Ynduráin, *Quantum Chromodynamics*, Springer-Verlag (1983), ISBN 0-387-11752-0;

35) N. Brown and N. Dorey, Mod. Phys. Lett. A **6** (1991) 317;

36) H. Pagels and S. Stokar, Phys. Rev. D **20** (1979) 2947;

37) R. Jackiw and K. Johnson, Phys. Rev. D **8** (1973) 2386.

SCHWINGER-DYSONOV PRISTUP I POOPĆENA IMPULSNA APROKSIMACIJA ZA $\pi^0\gamma^\star\gamma$ PRIJELAZ

Razmatramo faktor oblika prijelaza pion-foton u Schwinger-Dysonovom pristupu i impulsnoj aproksimaciji. Izlažemo rezultate za mnogo veće energije od sada dostupnih, do 36 GeV^2, i pokazujemo slaganje s asimptotički izvedenim ponašanjem, za koje također dajemo nov izvod. Raspravljamo kako mjerenja u Jefferson Labu mogu dati podatke o dinamičkom oblaganju kvarkova.